Density functional theory study of the Fourier transform infrared and Raman spectra of dichloro-bis(2,4-pentanedionate)tin(IV)

ARTICLE *in* SPECTROCHIMICA ACTA PART A MOLECULAR AND BIOMOLECULAR SPECTROSCOPY · JUNE 2001

Impact Factor: 2.35 · DOI: 10.1016/S1386-1425(00)00457-1 · Source: PubMed

ELSEVIER

Spectrochimica Acta Part A 57 (2001) 1149–1161

SPECTROCHIMICA ACTA PART A

www.elsevier.nl/locate/saa

Density functional theory study of the Fourier transform infrared and Raman spectra of dichloro-bis(2,4-pentanedionate)tin(IV)

Claudio A. Téllez S. [a,*], Eduardo Hollauer [a], M.I. Pais da Silva [b], M.A. Mondragón [c], I. Haiduc [d], M. Curtui [d]

[a] *Instituto de Química, Departamento de Físico-Química, Universidade Federal Fluminense (UFF), Morro do Valonguinho s/n, Niteroi-Centro, Cep 24210-150 Rio de Janeiro, Brazil*

[b] *Departamento de Química, Pontifícia Universidade Católica do Rio de Janeiro, PUC-Rio, R. Marqués de S. Vicente 225, Gávea, Cep 22453-900 Rio de Janeiro, Brazil*

[c] *Departamento de Física Aplicada y Tecnología Avanzada, Instituto de Física, UNAM, Apdo. Postal 0.1010, Querétaro, Qro 76001, Mexico*

[d] *Chemistry Department, Babes-Bolyai University, R-3400, Cluj-Napoca, Romania*

Received 19 September 2000; accepted 25 October 2000

Abstract

Fourier transform infrared and Fourier transform Raman spectra of dichloro-bis(2,4-pentanedionate)tin(IV) have been obtained. Density functional theory (DFT) BLYP calculations, have been carried out with the purpose of understanding the metal-ligand region spectra of this compound. Vibrational wavenumbers calculated by BLYP/6-31G* force fields are closed with the experimental results. The percentage of deviation of the bond lengths and bond angles gives a good picture of the normal modes, and serves as a basis for the assignment of the wavenumbers. The calculated geometrical parameters show slight differences compared with the experimental ones, and these differences can be explained by the different physical state of $Sn(acac)_2Cl_2$. The DFT-BLYP calculations assumed a free molecule in the gas phase. The experimental wavenumbers are obtained from the spectra of solid samples.

Keywords: Dichloro-bis(2,4-pentanedionate)tin(IV); Vibrational spectra; DFT-calculations.

1. Introduction

Previous studies on metal acetylacetonate complexes have been reported for quite some time [1–4] and Thorton's excellent review [5] summarizes the information available on acetylacetonate complexes up to 1990. Schönherr at al. [6] gives a short review on the works reported up to 1993, concerning the normal coordinate analysis and applied the Wilson-El'yashevich method [7–10] to obtain the normal vibrations of $(M(acac)Cl_4)$,

* Corresponding author. Tel.: +55-21-2745689.
E-mail address: claudio@risc1.gfq.uff.br (C.A. Téllez S.).

1386-1425/01/$ - see front matter
PII: S1386-1425(00)00457-1

M=Sn(IV), Sb(IV). Téllez and Gómez [11,12] carried out a vibrational study of uranyl 2,4-pentanedionate reporting the Fourier transform (FT) infrared and Raman spectra. In the study a normal coordinate analyses for the framework structure was carried out to aid the assignment of the spectral wavenumbers. For dihalo-bis(acetylacetonate)tin(IV) complexes, the stereochemistry, configuration rearrangements and vibrational spectra of $Sn(acac)_2Cl_2$ were studied by Jones and Fay [13], but we do not find in this work a complete interpretation of the infrared spectra. Faller and Davison [14] reported some infrared bands and Raman shifts of $Sn(acac)_2Cl_2$. The determination of the molecular structure of dichloro-bis(2,4-pentanedionate)tin(IV) was carried out by Miller and Schlemper [15], which revealed that $Sn(acac)_2Cl_2$ crystallizes in the monoclinic space group C_2/c with $Z=4$. Analyzing the published data about $Sn(acac)_2Cl_2$, we felt that it was necessary to carry out a rigorous study of the infrared and Raman spectra in the region 600–30 cm^{-1}, in which we found the framework and ligand vibrations together. To achieve this purpose our procedure was to obtain the FT-infrared and the FT-Raman spectra of solid $Sn(acac)_2Cl_2$ and its FT-Raman polarized spectra in solution of CH_2Cl_2. Since the density functional theory (DFT) predicts molecular structural parameters and spectral wavenumbers in good agreement with experimental results [16–18], we used it to aid in the vibrational assignment of $Sn(acac)_2Cl_2$.

2. Experimental

$Sn(acac)_2Cl_2$ was prepared by reaction of tin(IV) chloride and acetylacetone in chloroform as described by Dilthey [19]. With a Nicolet 950 FT-Raman spectrophotometer we recorded two series of Raman spectra for $Sn(acac)_2Cl_2$: one for the solid sample and the other for a solution of the solid sample in CH_2Cl_2 at 0 and 90° polarization. The conditions of the measurements were: scan number = 120; collection length of 20.904 s; resolution, 4; a laser frequency of 15.7982 cm^{-1}; interferogram peak position, 8192; and apodization, Happ–Genzel. The detector was of InGaAs; beamsplitter of CaF_2; aperture, 150; sample gain, 16; and Raman laser frequency of 9393.49 cm^{-1}. The conditions for the polarized Raman spectra were the same as above with the exception that the number of scans was of 600. The infrared measurements for the solid sample were carried out on a Perkin-Elmer 2000 FT–IR spectrometer. The data were collected with a 0.5 cm^{-1} interval with a resolution of 4 cm^{-1}. The scanning speed was 0.2 cm^{-1} and 120 scans were performed. The solid samples were measured in the range 4000–370 cm^{-1} as KBr pellets. Between 700 and 70 cm^{-1} the infrared spectrum was measured on a Nicolet 740 FT-IR spectrometer with a resolution of 0.3 cm^{-1}, using a deuterated tryglycine sulfate (DTGS) detector with a polyethylene windows, and an Ever-Glo™ mid-far IR (9600–50 cm^{-1}) source. In this case the sample was mixed with polyethylene powder and pressed to form a pellet. Figs. 1–5 illustrated the infrared and Raman spectra of $Sn(acac)_2Cl_2$.

3. Results and discussion

3.1. Structure

The X-ray experimental parameters for $Sn(acac)_2Cl_2$ were carried out by Miller and Schlemper [15]. The DFT-BLYP calculated structural parameters are comparable with the experimental ones. All the calculated bond lengths were found to be higher when compared with the experimental data. The experimental Sn–Cl bond distance of 2.345 Å gave a calculated increased 3.8% value of 2.434 Å, and the C_4–O_2 bond length with a experimental value of 1.275 Å gave a calculated value of 1.310 Å being 2.8% longer. Deviations in the bond angles from the corresponding experimental parameters are also quite small. The theoretical structural parameters correspond to a single free molecule, the X-ray experimental results were obtained from diffraction data of a solid sample. In the solid state $Sn(acac)_2Cl_2$ crystallizes in the monoclinic space group C_2/c with four molecules in the unitary cell, and the chloro ligands are in *cis* positions and are related

by a crystallographic 2-fold axis. The DFT calculated structure could be classified in the C_2 point group. A comparison between the experimental reported structural parameters and the DFT - BLYP calculated ones are given in Table 1.

3.2. Vibrational irreducible representation

According the C_2 symmetry for the $Sn(acac)_2Cl_2$ complex, the $3n-6=87$ vibrational modes can be classified among the symmetry species:

$$\Gamma_{vib} = 44A(IR,\ R) + 43B(IR,\ R)$$

3.3. Band assignments

The band assignments presented here obey the following criteria: (a) Comparison in some case with reported vibrational assignment of characteristic molecular groups and bonds found in differ-

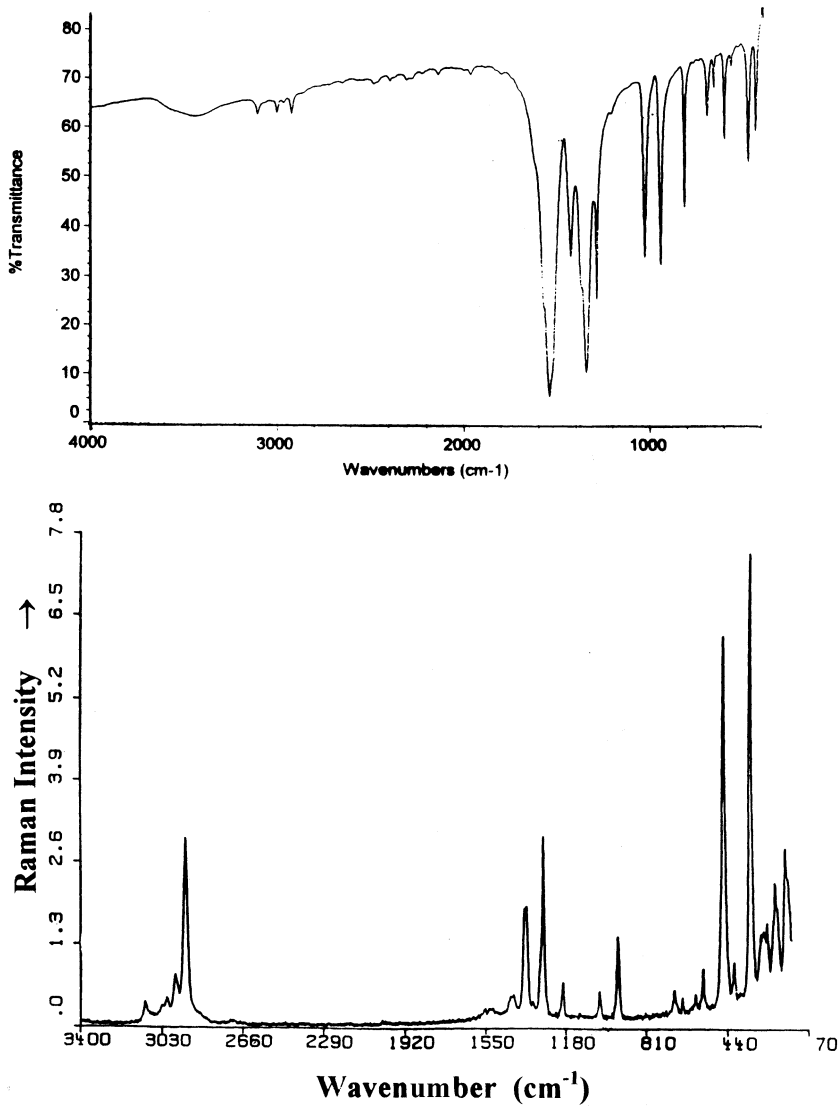

Fig. 1. FT-infrared and FT-Raman spectra of dichloro-bis(2,4-pentanedionate)tin (IV).

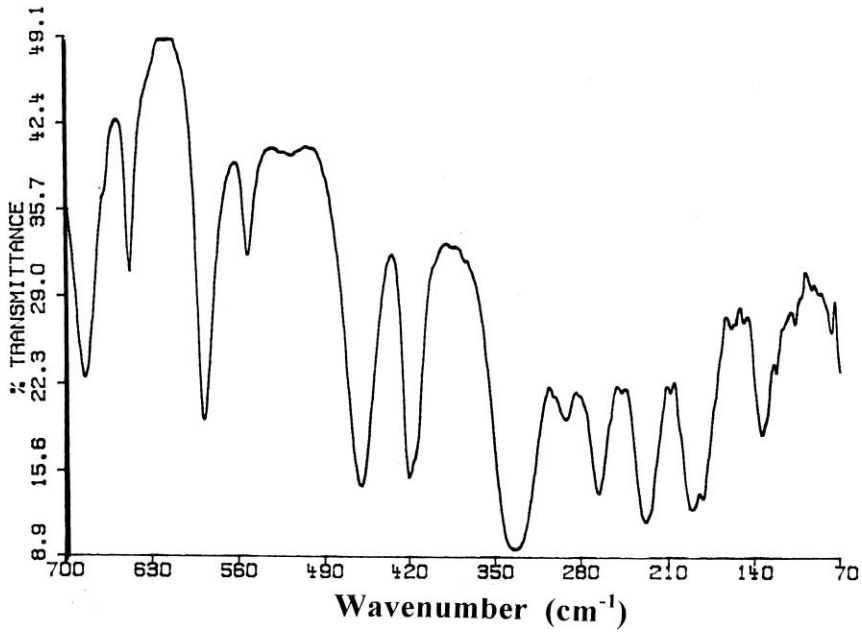

Fig. 2. FT-infrared spectrum of $Sn(acac)_2Cl_2$ in the region 700–70 cm^{-1}.

ent molecules. (b) The visual 3D computerized representation of the normal modes. (c) The Cartesian representation of the normal modes, in the absence of the potential energy distribution (PED), permits in the quantum mechanic ab initio DFT method, to study the distorted geometry of each mode. (d) Through the normal coordinate analysis for the SnO_4Cl_2 framework we obtained the PED.

3.3.1. Methyl group stretching and bending modes

The stretching ν(CH) infrared vibrational modes can be divided into 6A(IR, R) + 6B(IR, R) symmetry types.

In spite of the assignments of these vibrational modes being straightforward, we compared our observed IR bands with other 2,4-pentanedionate metal complexes. For Cu(II) 2,4-pentanedionate, Mikami et al. [20] assigned IR bands at 2987 and 2969 cm^{-1} to the b_{1u} and b_{2u} stretching ν(CH) modes. The band at 2985 cm^{-1} was attributed by the same authors to the b_{3u}-stretching mode. In a previous work on uranyl 2,4-pentanedionate [11,12], the observed wavenumbers at 2958 and 2925 cm^{-1} were assigned to the b_{1u} and b_{2u} ν(CH) stretching, and in the same complex, the band at 2855 cm^{-1} was assigned empirically to a b_{3u} ν(CH) stretching mode. For $Sn(acac)_2Cl_2$ we could not observe all the 12-infrared and Raman active stretching modes. In the infrared spectrum we observed only five bands, which can be correlated with the calculated DFT-B3LYP values. In the Raman spectrum we observed five bands also; four of them are coincident with their infrared counterpart. The calculated values show that six pairs of bands have practically the same wavenumber value, these finding agree with the experimental observation: bands must be overlapped. Our assignment for the observed infrared and Raman wavenumbers (cm^{-1}) corresponding to the A and B symmetry types of the C–H stretching are: 3061 (IR) (A), 3031(IR, R) (B), 3004 (IR, R) (B), 2967 (IR, R)(A), 2923 (IR, R)(A) and 2923 (IR, R)(A) cm^{-1}. For the Raman shift at 3034 cm^{-1}, assigned as ν(CH)(B), we have not found its infrared counterpart. For the infrared spectrum, no new C–H stretching band was found by analyzing the band deconvolution.

Four methyl groups give 24 bond angle bending internal co-ordinates, by means of them we can

described the δ(HCH) bending and $\rho(CH_3)$ rocking modes. Discarding the redundancy co-ordinates according the C_2 symmetry, the bending and rocking modes have the vibrational representation: $\Gamma_{HCH} = 6A(IR, R) + 6B(IR, R)$ and $\Gamma_\rho = 4A(IR, R) + 4B(IR, R)$. In the infrared spectrum only five δ(HCH), vibrational modes could be identified at 1557, 1539, 1518, and 1507 and 1439 cm^{-1}. The deconvolution analysis shows only two new bands at 1550 and 1522 cm^{-1}, which can be assigned as the δ(HCH) modes. In the Raman spectrum we find three coincident bands with the infrared spectrum at 1554, 1535 and 1517 cm^{-1}. The Raman band that was founded at 1521 has its infrared equivalent band identified in the deconvolution analysis, and for the Raman band at 1433, we did not found its infrared equivalent. The deconvolution analysis reveals two new bands in the infrared spectrum at 1550, 1522 cm^{-1}, and two new bands in the Raman spectrum at 1463 and 1429 cm^{-1}. The calculated DFT wavenumbers agree well with the experimental ones. For the rocking vibrations, only one infrared band centered at 1024 cm^{-1} could be assigned. Deconvolution analysis confirms two infrared absorptions at 1024 and at 1015 cm^{-1}. The base line for the band centered at 1024 cm^{-1} has a width of 80 cm^{-1}. In the 1104–1071 cm^{-1} region the calculated spectrum assigns eight rocking vibrations showing four pairs of overlapped bands.

3.4. Skeletal stretching ν(C=O), ν(C=C) or ν(O–C–C) vibrational mode

As we have pointed out in the discussion of the infrared and Raman spectra of uranyl 2,4-pentanedionate [11], for the ν(C=O) and ν(C=C) infrared stretching modes assuming a 'benzenoid resonance' structure of the ligands by coordination with the $SnCl_2$, we can consider equivalent internal co-ordinates for the C–O and C–C bonds. According to the C_2 experimental and calculated symmetry for the $Sn(acac)_2Cl_2$ complex, the vibrational infrared and Raman repre-

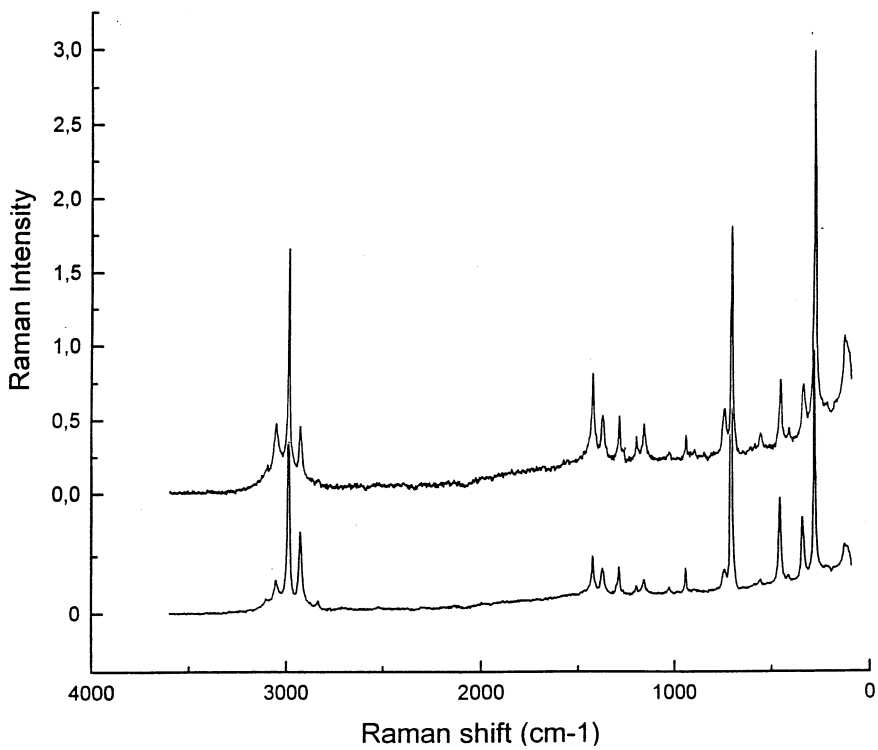

Fig. 3. FT-Raman polarized spectra of $Sn(acac)_2Cl_2$ in CH_2Cl_2.

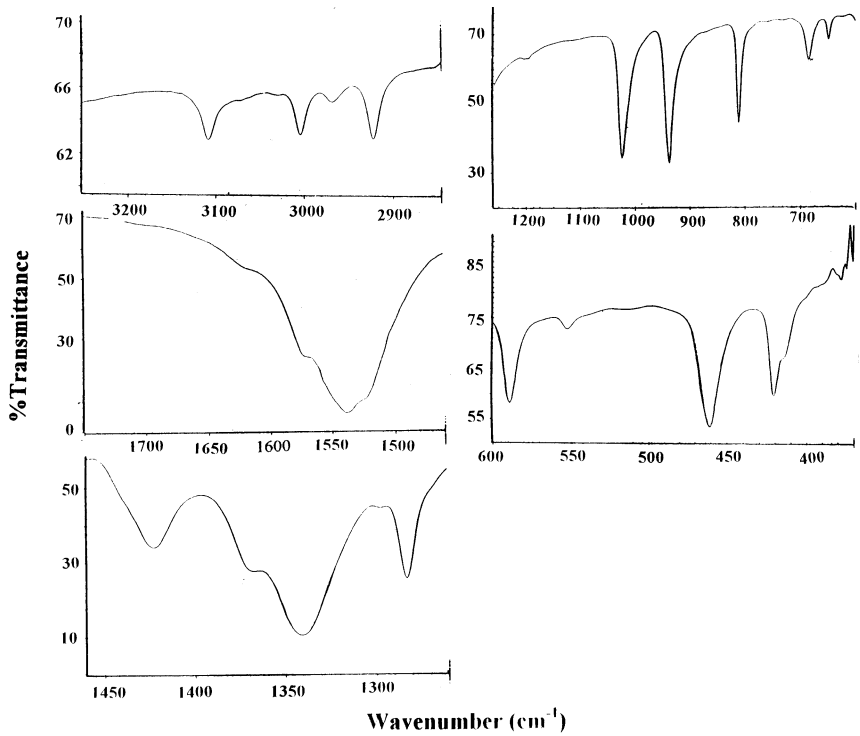

Fig. 4. FT-infrared spectrum of dichloro-bis(2,4-pentanedionate)tin(IV). Detailed regions.

sentations for the stretching of these bands are: $\Gamma_{C=O} = 2A + 2B$, $\Gamma_{C=C} = 2A + 2B$ and $\Gamma_{O-C-C} = 2A + 2B$. Since the C=O and C=C internal coordinates are together, more physically meaningful is to consider the O–C–C oscillator in the description of the normal mode. In the infrared spectrum we observed only two bands at 1620 and 1574 cm^{-1}. The deconvolution analysis also gives two absorption bands confirming the observed values. The calculated wavenumbers are found at 1597, 1597, and 1594 and 1581 cm^{-1}; two coincident peaks and the third one with a shift of 3 cm^{-1}. The fourth band has a shift of 16 cm^{-1} related to the first absorption band. The difference of intensity between the coincident bands is clear, and this overlap would predict the observations of only three absorption bands in the infrared spectrum in the region between 1630 and 1570 cm^{-1}. According to the description of the normal modes in Cartesian coordinates, the wavenumber found at 1597 cm^{-1}, corresponding to the observed band at 1620 cm^{-1}, can be assigned as the coupled mode: $\nu(C{=}C) + \delta(CCH) + \nu(CH)_{methine}$. The second band, with coincident wavenumbers which can be correlated with three observed band at 1620 cm^{-1}, can be assigned principally as $\nu(O–C–C) + \beta(HCH)$. The calculated value at 1594 cm^{-1} can be described as a very complex normal mode including principally ring bond distance distortions, external OCR ($R{=}CH_3$) bond angle distortion, HCH distortion and CH methine bond distance distortion. The most probable assignment for this mode is: $\nu(C{=}C) + \delta(OCR) + \beta(HCH)$.

3.4.1. $\nu(C–CH_3)$ stretching modes

Previous workers [2,21] have assigned bands at 960–930 cm^{-1} to $\nu(C–CH_3)$. For dichloro-bis(γ-acetylacetonate)platinum(II), Behnke and Nakamoto [22] based on a normal coordinate analysis pointed out that a strong coupling between the central $\nu(C–C)$ and the $\nu(C–CH_3)$ stretching modes exists. According to the potential energy distribution, these authors found that

the observed predominant 1350 cm^{-1} band $\nu(C-\dddot{}C)$ was strongly coupled with $\nu(C–CH_3)$. More pure $\nu(C–CH_3)$ character is attributed to the observed 901 cm^{-1} wavenumber ('a' species). For potassium dichloro(acetylacetonate)platinate (II) Behnke and Nakamoto [22] found that the observed wavenumber at 952 cm^{-1} has the $\nu(C–CH_3)$ (a_1) as predominant mode, and the observed wavenumber at 941 cm^{-1} can be assigned to the pure $\nu(C–CH_3)$ (b_2) mode. For $UO_2(acac)_2$ Nakamoto et al. [4] reported that the IR observed at the 1274 cm^{-1} wavenumber can be ascribed to the coupled mode $\nu(C{=}C) + \nu(C–CH_3)$, and the 925 cm^{-1} wavenumber should be the $\nu(C–CH_3)$ (b_{1u} and b_{2u}) stretching modes. Concerning the Raman spectrum experimental evidence for the assignment of the $\nu(C–CH_3)$ stretching modes using ^{13}C, was reported by Junge and Musso [3] for the Cu(II)–acetylacetonate complex. We have assigned in $UO_2(acac)_2$ [11] the Raman shifts found at 944 and 933 cm^{-1}. Continuing with the analysis, for the $Sn(acac)_2Cl_2$ complex, we observed two Raman bands at 986 (p) and 939 cm^{-1}. In the infrared spectrum we observed a band at 938 cm^{-1}. The deconvolution analysis confirms only the observed bands in both, the infrared and Raman spectra. The infrared band at 938 cm^{-1} with its Raman counterpart band observed at 939 cm^{-1}, can be assigned as the coupled mode $\nu(C–CH_3) + \nu(O-\dddot{}C-\dddot{}C)$. Concerning this assignment, the DFT calculations indicate two wavenumbers at 963 and 960 cm^{-1}.

3.4.2. *ν(C–H) methine stretching*

As we have pointed out in Refs. [11,12] it is expected that the vibrational wavenumber $\nu(C–H)$ stretching of the methine groups will be higher than those of the $\nu(C–H)$ methyl groups. The observed bands at 3108 (IR, R) cm^{-1} and at 3070 (IR) cm^{-1} can be assigned as the $\nu(C–H)$ methine group.

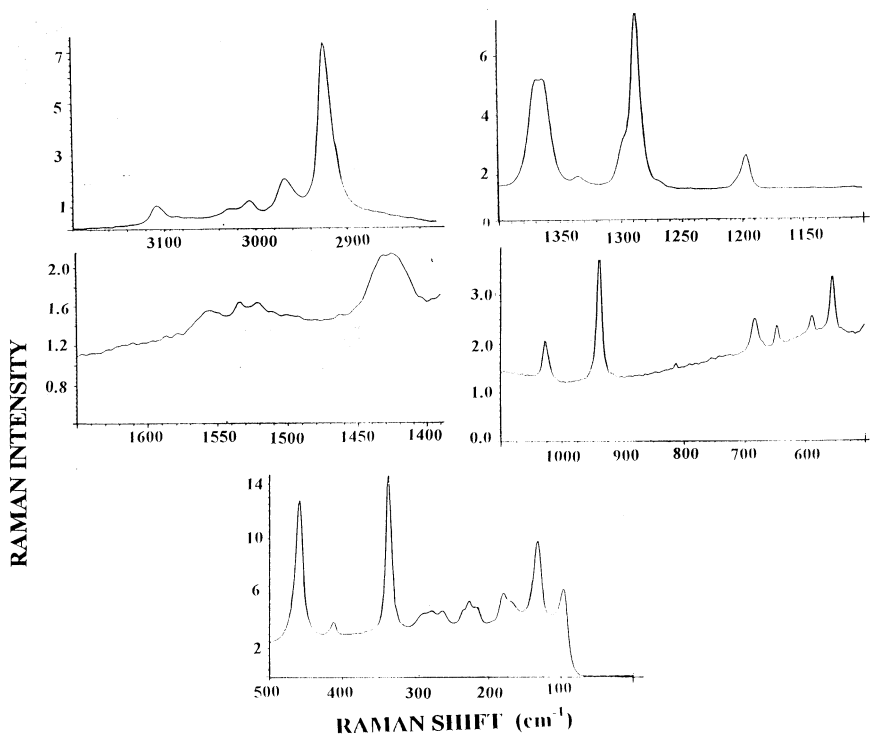

Fig. 5. FT-Raman spectrum of dichloro-bis(2,4-pentanedioante)tin(IV). Detailed regions.

Table 1
Bonds lengths and inter-bond angles for dichlorobis(2,4 pentanedionato)tin (IV)

Bond lengths (Å)			Bond angles (°)		
N°. atoms	Reference [14]	DFT/B3LYP	N°. atoms	Reference [14]	DFT/B3LYP
4-12	1.491	1.502	2-1-11	87.3(1)	86.51
4-6	1.397	1.402	3-1-10	84.0(1)	86.51
6-8	1.374	1.401	2-1-10	87.0(1)	84.19
3-5	1.275	1.310	16-1-17	96.86(5)	98.50
9-11	1.29	1.313	1-3-5	125.0(2)	130.42
1-2	2.064	2.101	1-11-9	124.5(2)	130.81
1-10	2.051	2.081	3-5-13	114.6(2)	114.61
1-16	2.345	2.434	5-7-9	125.0(2)	124.93
1-17	2.345	2.434	13-5-7	120.4(3)	120.99
12-20		1.096	5-7-9	125.9(3)	124.93
14-28		1.096	11-9-7	125.4(2)	124.59
12-22		1.092	11-9-15	114.4(3)	114.19
13-23		1.092	7-9-15	120.3(3)	121.22

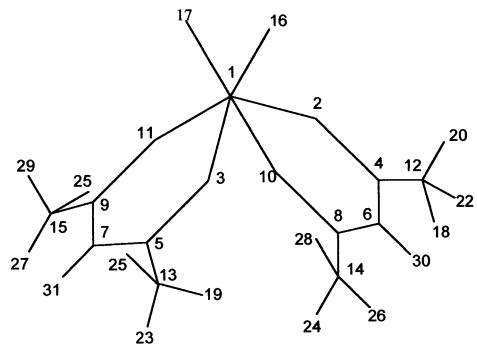

3.4.3. Bending in plane vibrations of the acetylacetonate ligands

Discarding six bond angle redundant coordinates, the vibrational representation for these normal modes is $\Gamma = 6A + 6B$, which can be subdivided as:

$\Gamma_{\alpha} = A + B$: α(O–Sn–O) bending deformations.

$\Gamma_{\beta} = 2A$

$+ 2B$: β(C–O–Sn or O–C–C)

bending deformations.

$\Gamma_{\gamma} = 2A$

$+ 2B$: γ(O–C–CH_3 or C–C–CH_3)

bending deformation.

$\Gamma_{\varepsilon} = A + B$: ε(C–C–H) bending deformations.

3.4.4. α(OSnO) bending vibrations

A rigorous analysis of the distorted geometry of these modes indicates that the 278 and 257 cm^{-1} calculated wavenumbers, which can be correlated with the experimental ones found at 292 (IR), 288 (R) cm^{-1} and 247 (IR), 238 (R, BCA) cm^{-1}, can be assigned as the coupled modes α(OSnO)(63%) + ν(SnO)(23%) and α(OSnO) + δ(OSnCl)(27%), respectively, where the percentage means the participation of the OSnO and OSnCl bond angles and the SnO bond distance.

3.4.5. β(COSn/OCC) ring angle bending deformations

Inside of the two asymmetric rings formed by the acetylacetonates ligands with the $SnCl_2$ we have twelve angle bending internal coordinates, in which, six of them are redundant coordinates, and two of the ring angle bending deformations were defined above as α(OSnO). The description of the four remaining β(COSn/OCC) vibrational modes is not easy due to the higher degree of coupling with other vibrational modes, principally with the

ring torsions. As a base for the assignment of these modes we studied the distorted geometry of each vibrational mode and we have determined the percentage of variation of the geometrical parameters. The results gives the following assignation: The polarized Raman band found at 986 cm^{-1} (975 cm^{-1}, calculated) can be assigned as the coupled mode β(OCC, CCC)(39%) + ν(O–C–C)(30%) + $\rho(CH_3)$(32%). The DFT calculated value of 972 cm^{-1} can be assigned to a very complex normal mode, which can be described as a ring deformation in which participate the O–C–C stretching in 26%, the internal ring bond angles OCC/CCC in 44%, and the rocking $\rho(CH_3)$ in 30%. The calculated value at 1581 cm^{-1}, corresponding to that experimental found at 1574 cm^{-1}, can be characterized principally for the O–C–C ring deformation and for the bending of the methyl groups. In a minor extension the internal CCC bond angles also participate. In the Raman spectrum only two very weak bands were observed at 1582 and 1574 cm^{-1}, which can be assigned to the OCC ring deformation.

3.4.6. γ(O–C–CH_3/C–C–CH_3) bending vibrations

The characterization of the four infrared and Raman active γ(O–C–CH_3/C–C–CH_3) bending modes, as modes without coupling, is without physically meaning, so these modes appear strongly coupled. Schönherr et al. [6] for $Sn(acac)Cl_4$, assigned in the infrared spectrum the bands found at 423 and 213 cm^{-1}, as the δ(CCMe) + δ(CCMe) and δ(CCMe) + $\sigma(Sn–Cl)_{op}$, coupled modes. The analysis of the distorted geometry raised for this kind of bending in the vibrational spectra of $Sn(acac)_2Cl_2$, pointed out the following probable assignment: 279(R) – 263(calc.) as $\delta(CCCH_3) + \tau(OCCC)\tau(CH_3)$; 265(IR), 263(R) – 259(calc) as $\delta(CCCH_3 + \tau(CCOSn) + \tau(CH_3)$; 209(IR), 217(R)–217(calc) as $\delta(CCCH_3) + \delta$(OSnCl/OSnO) + ν(SnO).

3.4.7. ε(C–C–H/O–C–H) bending vibrations

The infrared band found at 1423 cm^{-1} (14533 cm^{-1}, calculated), can de assigned as the ε(CCH) + β(HCH) coupled mode. The deconvolution band analysis shows the Raman band found at 1433 cm^{-1} and shows the other ε(CCH) + β(HCH) coupled mode at 1414 cm^{-1} (1419 cm^{-1}, calculated).

3.4.8. Out of plane bending and torsion modes

Among many possibilities to define torsion and out of plane angle bending internal coordinates, we have chosen the following: (i) Out of plane angle bending: four $\gamma(CO–C–CH_3\uparrow)$ for the methyl groups. Two θ(CC–C–H↑) for the –CH methine groups. (ii) Each ring formed by the binding of the ligands with $SnCl_2$ has six torsion axes, three torsion internal coordinates can be considered as redundant. The elected torsion coordinates are: two τ(O–Sn–O–C), two τ(C–C–C–CO) and two τ(Sn–O–C–C). The τ(C–C–C–O) and the τ(O–Sn–O–C) can be considered as a special case of a $\sigma((CH_3C)–C–C–O\uparrow)$ out of plane angle bending internal coordinate, such as that which we had earlier defined in Ref. [12]. The remain four torsion coordinates are ascribed for the methyl groups. Rotations of the methyl groups causes a variation of the dihedral angles found among the four atoms, which defines the internal coordinates.

The characterization of this torsion and out of plane angle bending modes using the DFT output of the normal modes is rather complicated. Here, for to obtain an approximate assignment of the normal mode, we used the computerized 3D visualization and the study of the distorted geometry of each mode.

Infared bands in the region 800–570 cm^{-1} were assigned to these out of plane vibrations. Here the two θ(CC–C–H) out of plane modes were calculated coincidentally at 852 cm^{-1}. The deconvolution band analysis of the Raman band found at 939 cm^{-1}, reveals two new bands at 879 and 860 cm^{-1} which can be assigned as pertaining to these θ(CC–C–H) modes. The observed infrared bands at 684, 664 and 648 cm^{-1} correlated with the DFT calculated values at 684, 664 and 672 cm^{-1} can be ascribed to the $\gamma(OC–C–CH_3\uparrow) + \sigma(CH_3C–C–O\uparrow)$ coupled modes. The other of these modes was observed in the Raman spectrum at 683 cm^{-1}. The two calculated wavenumbers at 170 cm^{-1} can be correlated with the observed values at 168 and 157 cm^{-1} in the Raman spectrum and can be assigned as the

Table 2
Comparison of the calculated DFT and infrared and Raman wavenumbers of $Sn(acac)_2Cl_2$

Sym.	DFT wn.	DFT I_{IR}[a]	DFT I_R[b]	ρ	IR wn.	IR (BCA)	R wn.	R (BCA)	Mode description
A	3248	2.30	126.2	0.17	3108	3109 (0.5)	3108		$\nu(CH)_{methine}$
B	3248	7.83	51.4	0.75	3070	3072 (1.0)	3108		$\nu(CH)_{methine}$
A	3168	6.42	66.2	0.74	3061				$\nu(CH)_{CH3}$
B	3168	15.9	48.0	0.75	3031	3032 (0.1)	3030		$\nu(CH)_{CH3}$
A	3167	5.8	40.0	0.73					$\nu(CH)_{CH3}$
B	3167	28.5	102.4	0.75			3024	3028 (4.9)	
B	3129	2.83	48.08	0.75	3004	3004 (0.6)	3005	3007 (7.3)	
A	3129	2.45	116.2	0.74					
A	3128	5.55	135.6	0.74	2967	2967 (0.5)	2966	2964 (21.8)	
B	3128	1.32	49.19	0.75					
A	3062	0.0	395.5	0.03	2923	2922 (0.8)	2922	2922 (120.0)	
B	3062	2.59	16.9	0.75					
B	3061	1.51	20.4	0.75					
A	3061	2.37	365.6	0.02	2923	2922 (0.8)	2922	2922 (120.0)	
B	1597	7.1	5.15	0.75	1620	1619 (4.9)			$\nu(C{=}C)+\beta(CCH)$
A	1597	334.1	5.97	0.11	1620				$\nu(C{:::}C{:::}O)$
A	1594	83.9	15.85	0.71					$\nu(C{:::}O)+\delta(OCR)+\beta(CCH)$
B	1581	585.5	9.47	0.75	1574	1573			$\nu(C{:::}C{:::}O)$
B	1526	14.0	2.69	0.75					$\beta(CCH)$
A	1525	3.93	4.79	0.74	1557	1557 (0.3)	1554	1555 (4.3)	$\beta(CCH)$
A	1516	86.6	14.42	0.74		1550 (13.0)			$\beta(CCH)$
B	1515	83.11	19.43	0.75	1539	1538 (18.0)	1535	1534 (1.6)	$\beta(CCH)$
A	1513	1.12	39.83	0.74		1522 (14.0)	1521	1521 (3.4)	$\beta(CCH)$
B	1512	105.8	11.82	0.75	1518		1517		$\beta(CCH)$
A	1512	0.77	28.5	0.74					$\beta(CCH)$
B	1512	115.4	4.35	0.75	1507	1509 (10.0)			$\beta(CCH)$
B	1454	10.17	5.93	0.75				1463 (0.1)	$\beta(CCH)$
A	1454	6.14	31.81	0.48	1439	1440 (0.4)			$\beta(CCH)$
A	1452	3.2	42.34	0.24			1433	1432 (4.9)	$\beta(CCH)$
B	1452	7.5	39.5	0.75				1429 (0.2)	$\beta(CCH)$
B	1433	446.5	0.80	0.75	1423	1423 (8.8)		1422 (1.3)	$\delta(CH)+\beta(CCH)$
A	1419	199.5	0.95	0.67				1414 (2.4)	$\delta(CH)+\beta(CCH)$
A	1341	30.5	27.05	0.25	1371	1371 (4.8)	1369p	1368 (49.0)	$\gamma(CCC)+\beta(CCH)$
B	1337	109.3	20.84	0.75	1340	1340		1334 (1.5)	$\gamma(CCC)+\beta(CCH)$
B	1242	0.73	1.54	0.75					$\delta(CCH)_{methine}$
A	1240	1.16	5.97	0.74	1282	1282 (0.1)	1286p	1290 (46.4)	$\delta(CCH)_{methine}$
A	1104	0.87	0.10	0.72					$\rho(CH_3)$
B	1104	0.72	0.05	0.75		1196 (0.1)	1195dp	1195 (8.3)	$\rho(CH_3)$
A	1097	27.93	0.94	0.66					$\rho(CH_3)$
B	1096	31.91	0.21	0.75			1155dp	1164 (0.2)	$\rho(CH_3)$
B	1080	3.98	0.56	0.75				1139 (1.0)	$\rho(CH_3)$
A	1080	4.51	1.54	0.74			1030p	1030	$\rho(CH_3)$
A	1073	18.02	5.00	0.38			1018p		$\rho(CH_3)$
B	1071	68.90	3.18	0.75	1024	1024 (3.5)		1026	$\rho(CH_3)$

Table 2 (*Continued*)

Sym.	DFT wn.	DFT I_{IR}[a]	DFT I_R[b]	ρ	IR wn.	IR (BCA)	R wn.	R (BCA)	Mode description
A	975	17.35	20.23	0.05			986p		Ring def. + $\rho(CH_3)$
B	972	61.39	5.09	0.75					δ(OCC/CCC) + ν(O::::C::::C) + $\rho(CH_3)$
B	963	413	0.17	0.75					ν(C–CH_3) + ν(O::::C::::C)
A	960	22.15	0.22	0.72	938	937 (6.8)	939	940 (28.1)	ν(C–CH_3) + ν(O::::C)
A	852	15.40	1.76	0.74				879 (2.1)	$\rho(CH)_{oop}$
B	852	12.5	0.71	0.75				860 (0.6)	$\rho(CH)_{oop}$
A	684	10.53	1.02	0.58	684	684 (1.5)			γ(OC–C–$CH_3\uparrow$) + ρ(H_3CC–C..O$\uparrow$)
B	682	2.03	1.58	0.75			683	683 (9.1)	γ(OC–C–$CH_3\uparrow$) + ρ(H_3CC–C..O$\uparrow$)
B	674	24.23	3.24	0.75	664				γ(OC–C–$CH_3\uparrow$) + ρ(H_3CC–C..O$\uparrow$)
A	672	1.98	2.77	0.74	648			646 (3.6)	γ(OC–C–$CH_3\uparrow$) + ρ(H_3CC–C..O$\uparrow$)
A	571	4.45	2.60	0.63	589		588	589 (4.6)	ν_s(SnO) + δ(OSnCl/OsnO)
B	570	14.39	0.98	0.75				571 (1.2)	ν_{as}(SnO) + δ(OSnO)
A	563	4.91	2.46	0.65					$\nu(SnO)_{short}$ + $\nu(SnO)_{long}$ + δ(OsnO)
B	561	12.21	1.92	0.75	552	552 (0.3)	554dp	554 (3.8)	ν_{as}(SnO) + δ(OSnCl)
B	452	31.05	1.93	0.75	460	460 (0.3)			δ(OsnO) + ν(SnO)
A	449	13.97	37.29	0.01			459p	460	ν_s(SnO) + δ(OSnO)
B	425	25.1	0.47	0.75	420	420 (0.6)			δ(OsnO) + δ(OSnCl)
A	421	18.16	1.63	0.63		415 (0.7)	411	412	δ(OsnCl) + δ(OSnO)
B	325	80.5	5.39	0.75	364				ν_{as}(SnCl) + ν(SnO) + δ(OSnCl/OsnO)
A	316	59.39	18.25	0.05	333		337p	337 (117.0)	ν_s(SnCl) + ν(SnO) + δ(OSnCl/OsnO)
B	278	43.10	0.57	0.75	292		288	292 (8.0)	δ(OsnO) + ν(SnO)
B	263	0.64	0.26	0.75			279	279 (19.0)	$\delta(CCCH_3)$
A	259	3.58	0.77	0.22	265		263	262 (13.0)	$\delta(CCCH_3)$
A	257	14.52	9.84	0.12	247			238 (4.4)	δ(OsnO) + δ(OSnCl)
A	229	1.15	3.82	0.64			234	230 (8.6)	δ(OsnCl) + δ(OSnO) + $\tau(CH_3)$
B	220	19.0	2.06	0.75	227		226	222 (19.0)	δ(OsnCl) + δ(OSnO)
A	217	7.61	4.89	0.18	209		217	212 (3.9)	$\delta(CCCH_3)$ + δ(OSnCl/OSnO)
B	197	22.88	0.30	0.75	191		195		δ(OsnCl) + δ(OSnO)
A	194	7.96	2.04	0.63	181		180	181 (17.0)	δ(OsnCl) + δ(OSnO)
B	184	3.95	0.53	0.75					ρ(H_3CC–C...O$\uparrow$)
A	170	0.12	1.37	0.74			168	169 (18.0)	χ(OCCC) + χ(SnOCC)
B	170	0.08	0.28	0.75			157		χ(OCCC) + χ(SnOCC)
A	118	4.57	3.22	0.74	133		133	133 (71.0)	δ(ClSnCl) + δ(OSnCl)
B	108	4.58	1.47	0.75	121				$\tau(CH_3)$ + δClSnCl)?
A	104	0.00	0.67	0.74	106				$\tau(CH_3)$ + skeletal bending
B	103	0.57	0.79	0.75				103 (22.0)	$\tau(CH_3)$ + skeletal bending
A	91	1.95	0.16	0.74			96	96 (38.0)	$\tau(CH_3)$
B	91	1.98	0.02	0.75				80 (0.5)	$\tau(CH_3)$
A	71	0.02	2.35	0.73	76				$\tau(CH_3)$
B	57	0.33	0.24	0.75					$\tau(CH_3)$
A	48	0.14	3.57	0.74					χ(OCCC) + χ(CCOSn)
B	35	2.52	3.21	0.75					χ(OsnOC) + χ(CCOSn)
A	28	3.03	3.90	0.74					χ(OCCC) + χ(SnOCC)

[a] Calculated infrared intensities (I_{IR}) are in kM/mol.
[b] Raman scattering activities (I_R) are in Å^4.amu.

coupled torsions: τ(OCCC)(61%) + τ(CCOSn) (26%), τ(OSnOC)(37%) + τ(CCOSn)(36%) + τ (OCCC)(25%), and τ(OCCC)(55%) + τ(SnCCC) (37%), where the percentages refer to the variation of the dihedral angle.

The wavenumbers found at 168 and 157 cm^{-1} in the Raman spectrum, can be assigned tentatively as $\rho(H_3C–C–C–O\uparrow) + \tau$(SnOCC). The remaining few observed bands in the low energy region 110–25 cm^{-1} of the infrared and Raman spectra can be assigned as torsion modes as we have described in Table 2.

3.4.9. Skeletal SnO_4Cl_2 vibrational modes

We can describe four Sn–O stretchings, two Sn–Cl stretchings, One Cl–Sn–Cl and one O–Sn–O angle bending, and the remaining seven angle bendings, defined as the mixture of the Δ(OSnCl) and Δ(OSnO) internal coordinates. The Jones and Fay [13] assignments for the framework of the Sn(acac)Cl_2 complex (values in cm^{-1}) was: 591: some ν(Sn–O); 461: ν(Sn–O); 334: ν(Sn–Cl); and 134: δ(ClSnCl). For the same Sn(IV) complex Faller and Davison [14] only list the experimental wavenumbers and they do not give any assignment. In Table 3 we present the framework assignments of the normal modes. Here we compared the results obtained by the DFT vibrational analysis, and those obtained by the traditional normal coordinate analysis (NCA). In the first case, as we do not have the PED to assist the vibrational assignment, we have studied for each skeletal mode the percentage of variation of the geometrical parameters through its Cartesian representation. This gives us an idea of which internal coordinate has a majority participation for the characterized the normal mode. In the NCA, as usual, the PED served as a basis for the vibrational assignment. The constraint in both procedures was limited to considering only the skeletal fragment. Both methods were coincident in the assignment.

3.4.10. Framework normal coordinate analysis (NCA)

A framework normal coordinate analysis was carried out using the traditional Wilson–El'Yashevich FG matricial method [7–10]. The purpose of the NCA was to assist the DFT-calculated and visual assignment of the low energy region of the infrared and Raman spectra of Sn(acac)$_2Cl_2$,

Table 3
Calculated and experimental wavenumbers for the SnO_4Cl_2 framework (C_s symmetry)[a]

Calc. (DFT)	Experimental	Assignment (DFT)	Assignment (NCA)
A 571	588(R), 589(IR)	ν_s(SnO)(48%)[b] + δ(OsnO/ClSnO)(31%)	ν_s(SnO)(90%)[c]
449	459 (R)	ν_s(SnO)(57%) + δ(OSnO)(16%)	ν_s(SnO)(98%)
421	411(R)	δ(OSnO)(38%) + δ(OsnCl)(34%)	δ(OsnO)(46%) + ν(SnCl)(31%)
316	337(R), 333(IR)	ν(SnCl)(35%) + δ(OSnO)(23%)	ν(SnCl)(64%) + δ(OSnO)(36%)
257	238(R), 247(IR)	δ(OSnO)(32%) + δOSnCl)(27%)	δ(OsnCl/OsnO)(97%)
229	234(R), 247 (IR)	δ(OSnCl/OsnO)(58%) + ν(SnO)(35%)	δ(OsnCl/OsnO)(88%)
194	180(R), 181(IR)	δ(OSnCl/OsnO)(34%) + ν(SnO)(30%)	δ(ClSnCl)(62%) + δ(OSnO)(35%)
118	133(R, IR)	δ(ClSnCl)(34%) + δ(OSnCl)(30%)	δ(OsnCl/OsnO)(93%)
B 570	571(R, BCA)	ν(SnO)(56%) + δ(OSnO)(20%)	ν(SnO)(97%)
452	460(IR)	ν(SnO)(52%) + δ(OSnO)(38%)	ν(SnO)(75%) + ν(SnCl)(20%)
425	420(IR)	δ(OSnCl/OsnO)(64%) + ν(SnO)(23%)	δ(OSnCl)(61%) + ν(SnCl)(29%)
325	364(IR)	ν(SnCl)(37%) + δ(OSnCl)(27%) + δ(OSnO)(20%)	ν(SnCl)(45%) + δ(OSnCl)(38%)
278	292(IR), 288(R)	δ(OSnO)(63%) + ν(SnO)(31%)	δ(OSnCl/OSnO)(90%)
220	227(IR), 226(R)	δ(OSnCl/OsnO)(60%) + ν(SnO)(30%)	δ(OSnCl/OSnO)(99%)
197	191(IR), 195(R)	δ(OSnCl/OsnO)(89%)	δ(OSnCl/OSnO)(99%)

[a] Units in cm^{-1}.
[b] % For the DFT assignment means the percentage of deviation of the bond stretching and bond angle.
[c] % For NCA means the PED.

where a considerable mixture of skeletal or framework SnO_4Cl_2 vibrational modes exist, with ligands and ligands–framework coupled modes. Geometrical parameters, which describe the skeletal structure of $Sn(acac)_2Cl_2$, are taken from Table 1. The symmetry coordinates, which describe the framework vibrations, were adapted from the description given in Ref. [12]. A modified general valence force field (MGVFF) potential function was used and the initial set of force constants was calculated from the relation $F_{ii} = \lambda_{ii}/G_{ii}$. The agreement between the observed and calculated wavenumbers is within 0.1%. The PED has revealed similar coupling as those predicted by the DFT method.

Acknowledgements

CATS thanks CNPq for the financial assistance from a research grant. Thanks are extended to Professor Dr José Walkimar de Carneiro Mesquita for kindly allowing the DFT calculations that were carried out on his computer facilities. E H also thanks FAPERJ and CNPq for the project grants.

References

[1] K. Nakamoto, A.E. Martell, J. Chem. Phys. 32 (1960) 588.
[2] K. Nakamoto, P.J. McCarthy, A. Ruby, A.E. Martell, J. Am. Chem. Soc. 83 (1961) 1066.
[3] H. Junge, H. Musso, Spectrochim. Acta 24A (1968) 1219.
[4] K. Nakamoto, Y. Morimoto, A.E. Martell, J. Am. Chem. Soc. 83 (1961) 4533.
[5] D.A. Thorton, Coord. Chem. Rev. 104 (1990) 173.
[6] T. Schönherr, U. Rosellen, H.H. Schmidtke, Spectrochim. Acta 49A (1993) 357.
[7] M.A. El'yashevich, Dokl. AN SSSR 28 (1940) 605.
[8] M.A. El'yashevich, Zh. Fiz. Khim. 14 (1940) 1381.
[9] E.B. Wilson, J. Decius, P.C. Cross, Molecular Vibrations, the Theory of Infrared and Raman Vibrational Spectra, McGraw-Hill, New York, 1955.
[10] D.E. Mann, T. Shimanouchi, J.H. Meal, L. Fano, J. Chem. Phys. 27 (1957) 213.
[11] S.C. Téllez, J. Gómez Lara, Spectrochim. Acta 51A (3) (1995) 395.
[12] S.C.A. Téllez, J. Gómez Lara, Spectrosc. Lett. 27 (2) (1994) 209.
[13] R.W. Jones Jr, R.C. Fay, Inorg. Chem. 12 (11) (1973) 2599.
[14] J.W. Faller, A. Davison, Inorg. Chem. 6 (1) (1967) 182.
[15] G.A. Miller, E.O. Schlemper, Inorg. Chim. Acta 30 (1978) 131.
[16] R.G. Parr, W. Yang, Density-Functional Theory of Atoms and Molecules, Oxford University Press, London, 1989.
[17] A.D. Becke, J. Chem. Phys 98 (1993) 1372.
[18] C. Lee, W. Yang, R.G. Parr, Phys. Rev. B 37 (1988) 785.
[19] W. Dilthey, Ber. Deut. Chem. Ges. 36 (1903) 923.
[20] M. Mikami, I. Nakagawa, T. Shimanouchi, Spectrochim. Acta 23A (1967) 1037.
[21] R. Mecke, E. Funck, Z. Elektrochem. Ber. Bunsenges. Phys. Chem. 60 (1956) 1124.
[22] G.T. Behnke, K. Nakamoto, Inorg. Chem. 6 (3) (1967) 433.